DEVELOPMENT OF cm-SCALE WALL CLIMBING HEXAPOD ROBOT WITH CLAWS

Mayo Funatsu, Yushi Kawasaki, Soichiro Kawasaki, Koki Kikuchi,
Department of Advanced Robotics, Chiba Institute of Technology Chiba, Japan

e-mail: kikut@ieee.org

In this paper, we investigate the slip condition on a vertical wall surface and propose a cm-scale hexapod robot with claws that can climb the vertical wall. Since the volume force such as gravity is proportional to the length cubed and the area force such as muscle force is proportional to its cross section, i.e., the length squared, an object is more capable of overcoming gravity the smaller it is. This scaling effect allows a small robot to fly easily, accelerate rapidly, and climb a vertical wall with minimal difficulty. Here we developed a claw-type hexapod robot with a body length of 8.5 cm and weight of 13.5 g and realized horizontal and vertical locomotion on a vertical wall. In addition, we clarified the relationship between the gripping ability of the claws and the surface properties of the wall using a mathematical model.

Keywords:
vertical wall climbing, scaling effect, hexapod robot, claws, slip condition

1. Introduction

Since vertical wall traversability is important for robotic operations such as window cleaning and maintenance of tall buildings, various wall adsorption mechanisms have been proposed and developed [Goran 2009, Hirose 1992, Kathryn 2008, Miyake 2008, Murphy 2007, Yoneda 2001]. A suction cup using an electric vacuum pump generates a large adsorption force by exerting negative pressure on the cup surface [Yoneda 2001, Miyake 2008] and allows a robot to locomote even upside down on a ceiling,but this makes whole system large andincreases the robot's risk of falling. A passive adhesive disc such as an octopus sucker also generates large adsorption force and makes a systemsmall and simple, but this requires a mechanism for controlling the peeling force and is only operable on smooth surfaces [Murphy 2007]. An electromagnetic system, as used in window cleaning for example, is also useful [Hirose 1992], but itsweight limits its range of operation environments.

Due to the scaling effect, a small robot has great advantages for climbing vertical walls. Small objectssuch as insects can easily overcome gravitybecause gravity is a volume force that is proportional to mass, which is proportional to the length cubed. Furthermore, muscle is anarea force proportional to its cross-section. Therefore, the smaller the object, the larger the area force per volume force, resulting in a higher muscle force to body weight ratio. This meanscm-scale insectshave a force to body weight ratio a hundredfold greater than that of m-scale animals. This same scaling effect is true of a cm-scale robot compared with am-scale robot. Using this concept, several adhesion systems for a small wall climbing robot have been proposed and developed [Birkmeyer 2011, Kawasaki 2014, Kim 2008, Suzuki 2010, Unver 2010]. The sticky structure based on the Van der Waals force used by a gecko is not strongly limited by surface environment and is promising, but requires high MEMS technology to fabricate [Kim 2008]. Claws, such as those of a beetle, allow a small and simple system, but they cannot be used for locomotion on a smooth surface such as glass [Birkmeyer 2011]. The wet adhesion used by an ant, for example, is extremely promising for mm-scale or μm-scale, but it is still difficult to implement such a system for a robot because of the weight limitation imposed by sensor devices, etc. [Suzuki 2010]. As mentioned above, although several mechanisms have been studied, a simple wallclimbing robot based on the scaling effect, e.g., thecm-scale (for example, less than 10cm), has not yet been realized.

From this point of view, we focus on the distributed operation on concrete walls of high buildings by many small robots and develop a cm-scale vertical wallclimbing robot. The robot has six legs with claws and moves horizontally and vertically on the wall surface. Here we investigate the relationship between the grip bythe claw of the leg and the surface properties of the wall using both a mathematical model and an experimental result to realize locomotion on the vertical wall.

2. Hexapod robot with claws

2.1 Robotic system overview

Figure 1 shows the proposed wallclimbing six-legged (hexapod) robot. The body length and width are 8.5cm, the height is 3.5cm, and the weight is 13.5g. The robot includes a battery(lithium polymer: 3.7V, 90mAh, 2.8g). The robot consists of an upper body (the area enclosed by a red dashed line in Fig. 1) and a lower body which slide for traveling. The bodies are slid by a linear servomotor. Each body has three legs which are arranged every 120deg and driven by a shape memory alloy (SMA) spring (BMX100, TOKI Corp.).Two sets of directional claw units with four claws are mounted on each leg (the area enclosed by a black dashed line in Fig. 1). Hence, the robot has a total of two bodies, six legs, 12 claw units, and 48 claws. To grip the rough wall surface with high probability, the number of claw and the leg assignment were determined through the pilot experiments. Meanwhile,the robot has a total of 13 degrees of freedom (DOF) for body slide and up-and-down motions of the six legs, which are autonomously controlled by a Peripheral Interface Controller (PIC).

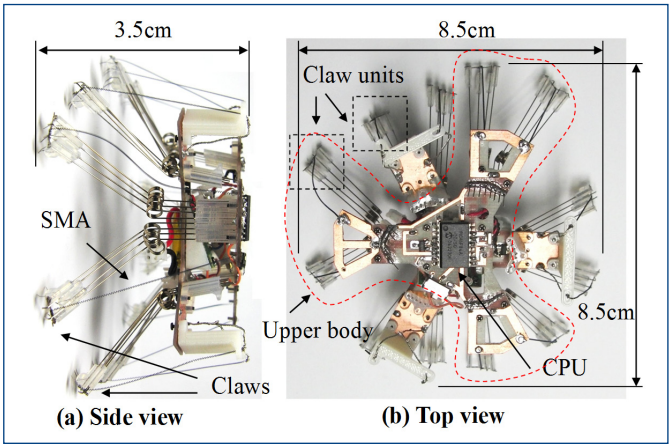

Figure 1. *Fabricated wallclimbing hexapod robot*

2.2 Locomotion mechanism

For vertical wall climbing, not only the adsorption force but also the rotational moment is very important. In bipedal locomotion, in which the center of mass (COM) is far from the wall surface, it is difficult to cancel the pitching moment. Even in quadruped locomotion, in which the COM is near the wall surface, it is difficult to cancel the pitching moment formotion such as the trot gait. Since the crawl gait is a static walk and always supported by three legs, the posture can be stabilized. However, control of the COM movement is still problematic during the transition between supporting and swinging leg phases. Consequently, we adopted a tripod gait by the hexapod robot in this study. Figure 2 illustrates the thrust mechanism that generates the COM approach near the wall surface. Figure 3 illustrates the supporting and swinging leg motions. The SMA spring pulls the legs by electrically heating and

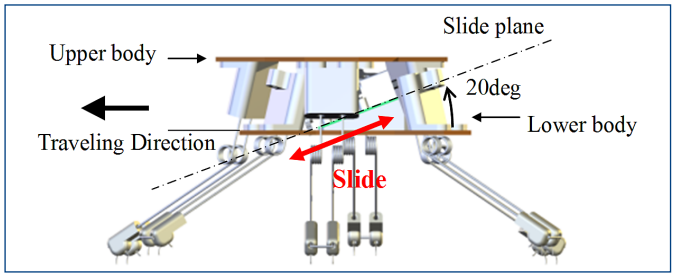

Figure 2. *Thrust mechanism which always pushes the claws during the swinging down phase*

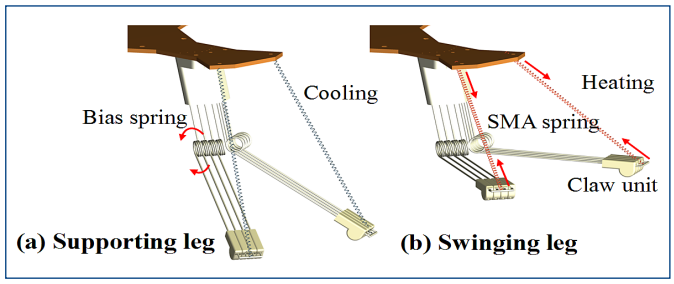

Figure 3. *Two-unit leg motion by a SMA and four bias springs*

the bias spring brings the legs back by naturally cooling the SMA spring. The thrust mechanism inclining 20deg in the direction of travel can always push the claws to the wall during the swinging down phase and raise the body during the swinging up phase. The movement of the COM perpendicular to the wall is 3mm (8.6% of the body height).

Note that the CPU is PIC16F84A and controls the tripod gait by pulse width modulation (PWM). The walking cycle was set at 18.4s based mainly on the SMA spring response for cooling.

3. Surface roughness and absorption models

3.1 Surface roughness model and its definition

In this section, we model the surface roughness of a concrete wall and analyze its relationship with the gripping force of the claw leg. First, to quantify the roughness, we fabricated a concrete wall model (stone powder clay consisting of La Doll PREMIX, PADICO). The wall was molded by disc paper to match the standardized roughness of the grain size established by Japan Industrial Standards (JIS). Figure 4 illustrates two types of surface models: (a) convex and (b) concave walls, and the claw condition. According to the pilot climbing experiments, it was difficult even for a beetle to climb on the convex type wall, because the condition in case (a) is not stable and caused its legs to slip. On the other hand, the condition in case (b) was relatively stable and the legs do not easily slip horizontally. In addition, the industrial concrete wall has many holes and is almost similar to the concave type. Thus, we focused on the concave type wall in this paper. Figure 5 shows the enlarged view of the concave type roughness of the fabricated wall and its mathematical model, which is defined as a hole of diameter d and offset h. Here, we consider the grain angle between the tangent of the hole and the line

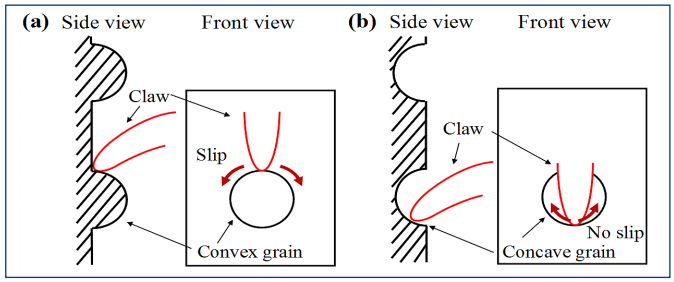

Figure 4. *Relationship between wall surface shape and claw position: (a) convex and (b) concave walls*

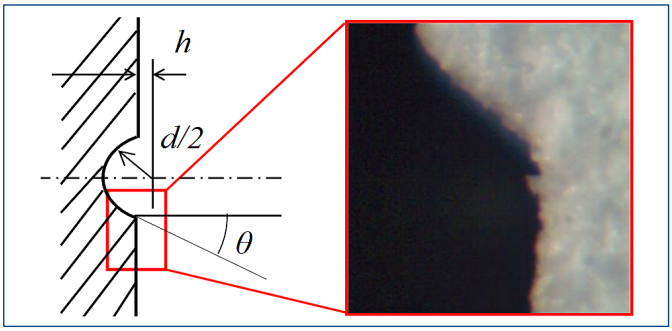

Figure 5. *Mathematical model of the hole and an image of the fabricated concave type surface roughness of the wall*

perpendicular to the wall surface, θ , as the representative indexand discuss the climbing success rate. Table 1 shows the grain size used in the experiments, the JIS defined grain diameter, and the grain angle actually obtained. The values given in parentheses are the standard deviation. Since several grains combine in various holes, the standard deviation is large. Note that P12 means a grain size of No. 12 and an average grain angle of 17 deg. In other words, the greater the number, the smaller the hole diameter and the smoother the wall surface. The hole number and position are arranged randomly.

	P12	P14	P16	P24	P30
d [mm]	1.4	1.2	1.0	0.6	0.5
σ [deg]	17 (18)	25 (15)	32 (22)	36 (11)	41 (10)

Table 1. *Grain size and grain angle*

3.2 Adsorption model analysis

In this paper, we simplify the hexapod robot into a 2D model that treats the radial six legs as upper and lower legs, i.e., as two legs, and we calculate the equations of equilibrium for gripping the wall. Fig. 6 illustrates the relationship between the forces exerted when statically gripping the wall. Here, the arc of the holes is deformed as the tangent for simplification and θ is the grain angle defined in Section 3.1 ($0 \le \theta < \pi/2$). The equations of equilibrium for gripping are as follows:

$$\begin{aligned}
&(F_1+F_2)\sin\theta+(-W_1+W_2)\cos\theta=0\\
&(F_1-F_2)\cos\theta+(W_1+W_2)\sin\theta-mg=0\\
&(-F_1+F_2)\sin(\alpha+\theta)+(W_1+W_2)\cos(\alpha+\theta)=0\\
&F_1\sin(\alpha+\theta)-W_1\cos(\alpha+\theta)=\frac{\tau}{R}
\end{aligned} \quad (1)$$

where F_i is the reaction force from the wall (F_i>0), W_i is the friction between the claw and the wall surface, m is the mass of the robot, g is the constant of gravity, α is the leg arrangement angle ($0 < \alpha < \pi/2$), R is the length of the leg, and τ is the torque of the pinchforce. Additionally, i=1 means the upper leg and i=2 means the lower leg. The origin of the coordinates is the COM of the robot and the third equation is the moment around the COM. Simple geometry reveals that $0 < \alpha + \theta < \pi/2$. From these equations, we obtain

$$\begin{aligned}
F_1&=\frac{\cos\theta}{\sin\alpha}\frac{\tau}{R}+\frac{\cos(\alpha+\theta)}{2\cos\alpha}mg\\
F_2&=\frac{\cos\theta}{\sin\alpha}\frac{\tau}{R}-\frac{\cos(\alpha+\theta)}{2\cos\alpha}mg\\
W_1&=\frac{\sin\theta}{\sin\alpha}\frac{\tau}{R}+\frac{\sin(\alpha+\theta)}{2\cos\alpha}mg\\
W_2&=-\frac{\sin\theta}{\sin\alpha}\frac{\tau}{R}+\frac{\sin(\alpha+\theta)}{2\cos\alpha}mg
\end{aligned} \quad (2)$$

From F_2>0, the following condition is obtained,

$$\frac{\tau}{Rmg} > \frac{\cos(\alpha+\theta)\tan\alpha}{2\cos\theta} \equiv K_{(\theta)} > 0, \tag{3}$$

where $\tau/(Rmg)$ indicates the pinch force tobody weight ratio. Hence, the smaller the body, the larger this value is. Since muscle force and body weight are proportional to cross-sectional area and volume, respectively, this equation implies that smaller robots have an advantage.

The slip conditions for the claws of the upper and lower legs are written as

$$\begin{aligned} \mu F_1 &\geq W_1 \\ \mu F_2 &\geq |W_2| \end{aligned}, \tag{4}$$

where μ is the coefficient of friction. The sign of the absolute value implies the direction of friction, i.e., the slip direction of the leg. From Eq. (2), W_1 is always positive.

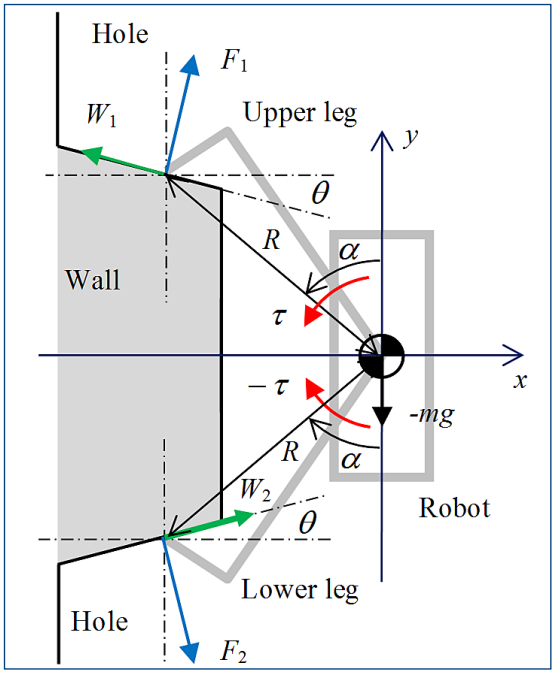

Figure 6. *Simplified mathematical model for wall gripping*

Case A: The claw of the upper leg does not slip.

From Eqs. (2) and (4), the condition that the claw of the upper leg does not slip is described as

$$(\mu - \tan\theta)\frac{\tau}{Rmg} \geq (\tan(\alpha+\theta) - \mu)K_{(\theta)}. \tag{5}$$

From the geometric condition of $\tan(\alpha+\theta) > \tan\theta \geq 0$ in Eqs. (3) and (5), the slip conditions for the upper leg are written as

$$\begin{aligned} &\mu - \tan\theta > 0 \\ &\frac{\tau}{Rmg} \geq \begin{cases} P_{(\theta)}K_{(\theta)} & if\ P_{(\theta)} \geq 1 \\ K_{(\theta)} & else \end{cases}. \\ &here\ P_{(\theta)} \equiv \frac{\tan(\alpha+\theta)-\mu}{\mu-\tan\theta} \end{aligned} \tag{6}$$

Thus, the claw of the upper leg does not slip, if and only if Eq. (6) holds.

Case B: The lower leg does not slip.

From Eqs. (2) and (4), the condition that the claw of the lower leg does not slip is described as

$$\begin{aligned} &\frac{\tau}{Rmg} \geq \frac{\mu+\tan(\alpha+\theta)}{\mu+\tan\theta}K_{(\theta)} \quad if\ W_2 \geq 0 \\ &(\mu-\tan\theta)\frac{\tau}{Rmg} \geq (\mu-\tan(\alpha+\theta))K_{(\theta)} \quad if\ W_2 < 0 \end{aligned}. \tag{7}$$

Here, by letting W_2=0, the following equation is obtained.

$$\frac{\tau}{Rmg} = \frac{\sin(\alpha+\theta)\tan\alpha}{2\sin\theta} \equiv J_{(\theta)} \tag{8}$$

This is the threshold for the slip direction for the lower leg. The first condition in Eq.(7) that the claw of the lower leg does not slip in the direction of the wall provides

$$\frac{\tau}{Rmg} \geq \frac{\mu+\tan(\alpha+\theta)}{\mu+\tan\theta}K_{(\theta)} \quad if\ J_{(\theta)} \geq \frac{\tau}{Rmg}, \tag{9}$$

while the second condition in Eq.(7) that the claw of the lower leg does not slip in the inverse direction of the wall provides

$$\begin{aligned} &\left[\mu - \tan\theta > 0, \frac{\tau}{Rmg} \geq \begin{cases} -P_{(\theta)}K_{(\theta)} & if\ -P_{(\theta)} \geq 1 \\ K_{(\theta)} & else \end{cases}\right] or \\ &\left[\mu - \tan\theta < 0, -P_{(\theta)}K_{(\theta} \geq \frac{\tau}{Rmg} > K_{(\theta)}\right] if\ J_{(\theta)} < \frac{\tau}{Rmg} \end{aligned}. \tag{10}$$

However, the second condition in Eq.(10) is always neglected, because the condition in Eq. (6) is more restrictive. Additionally, the first condition is almost neglected because the condition $\mu > \tan(\alpha+\theta)$ is rare. From the above discussion, the claw of the leg does not slip and the robot stays on the wall if and only if the conditions of Eqs. (6) and (10) hold.

3.3 An example of the numerical analysis

We introduce an example of the numerical analysis in this section. Figure 7 shows the areas expressed by the conditions in Eqs. (6) and (10), where the claw does not slip on the vertical wall. The parameters are as follows: μ=0.65 (obtained by the pilot experiment), m=13.5 [g], R=5 [cm], α=35 [deg], and g=9.8 [m/s^2]. The maximum pinch force to body weight ratio exerted by one leg is approximately 1.5, since the tension of the SMA spring is almost 0.02N. Since the robot uses every set of the three radial claw units for locomotion, the maximum pinch force to body weight ratio is approximately 3. This is extremely large compared with that of a human athlete. The gray area in Fig. 7(a) shows the condition that the claw of the upper leg does not slip. No any large pinch force stays the leg on the vertical wall in the condition of $\tan\theta > \mu$. The gray area in Fig. 7(b) shows the condition that the claw of the lower leg does not slip. This area is divided into two regions based on the slip direction (that is, the thin dashed line,

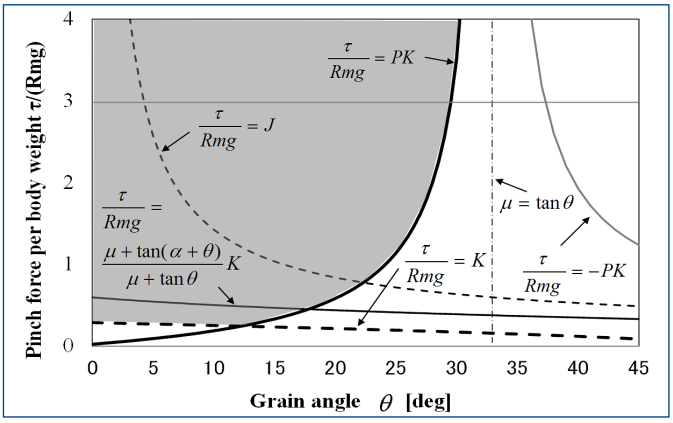

(a) *The area where the claw of the upper leg does not slip*

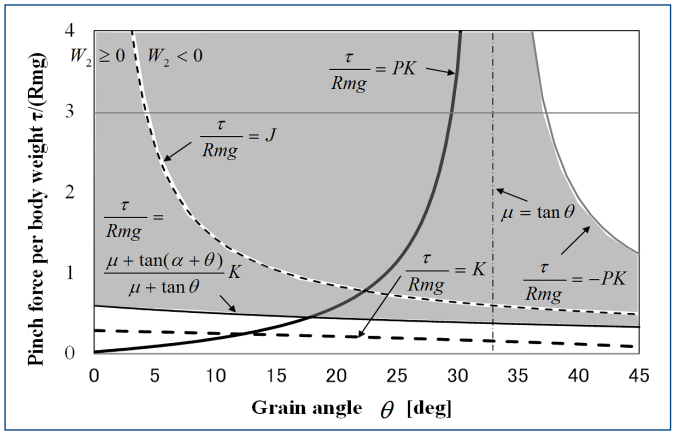

(b) The area where the claw of the lower leg does not slip

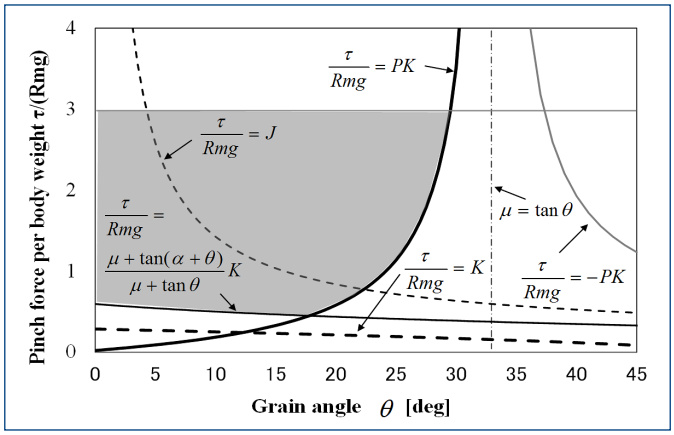

(c) The area where the robot stays on the vertical wall

Figure 7. *An example of the non-slip area: α=35[deg]*

Eq. (8)). Too small pinch force below the thin dashed line makes the leg slip in the direction of the wall, while too large pinch force above the thin dashed line makes it slip in the inverse direction of the wall. Eventually, the gray area in Fig. 7(c) shows the condition that the robot can stay on the vertical wall. This area is restricted by the upper and lower slip conditions and the maximum pinch force to body weight ratio. We find that the maximum grain angle on which the robot can climb on the vertical wall is almost 30deg (grain size of P14).

For the purpose of comparison, Fig. 8 shows the area that the robot can stay on the vertical wall in the case of α=20[deg]. We can see that the size of the gray area increases. According to the decrease of α, as the COM of the robot approaches the wall, the peeling moment decreases and the required pinch force becomes small. The minimum pinch force to body weight ratio required in the case of α=20[deg] also decreases compared with that in the case of α=35[deg]. Hence, the COM position is an important design consideration. Claw style vertical wall climbing is very difficult for m-scale robots, because the pinch force to body weight ratio is almost less than 1 which reduces the gray area. On the other hand, a cm-scale robot is not strongly affected by the pinch force; the friction coefficient with the wall is a more important factor. If the coefficient of friction becomes large, the chain dashed lines in Figs. 7 and 8 shift right and enlarge the gray area. Hence, miniaturization is an important design principle for a vertical wall climbing robot.

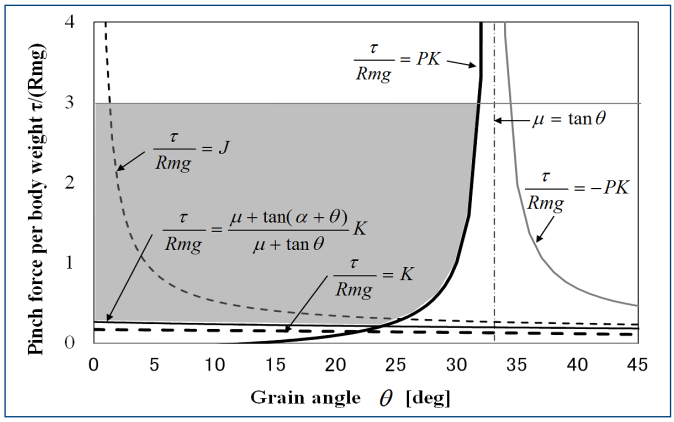

Figure 8. *An example of the non-slip area: α=20 [deg]*

4. Wallclimbing experiments

Based on the above analysis, we performed horizontal and vertical movement experiments on the vertical stone powder clay wall with grain sizes of P12, P14, P16, P24, and P30. Table 2 shows the results. Here we define a case in which the robot locomoted for more than 60 seconds as "OK" and the others as "NG". The robot climbed up and down and traveled horizontally on the vertical wall with a grain size of P12 and P14, i.e., a grain angle of 17deg and 25deg. The robot did not locomote on the vertical wall with a grain size of P16, P24, and P30, i.e., a grain angle of more than 30deg. This result is consistent with the numerical analysis in Section 3.3. Fig. 9 shows the stroboscopic pictures of the robot climbing on the vertical wall with the concave surface of P12 for 120s. The average velocities of climbing up,

	P12	P14	P16	P24	P30
Climbing up	OK	OK	NG	NG	NG
Climbing down	OK	OK	NG	NG	NG
Horizontal travel	OK	OK	NG	NG	NG

Table 2. *Experimental results for wall climbing*

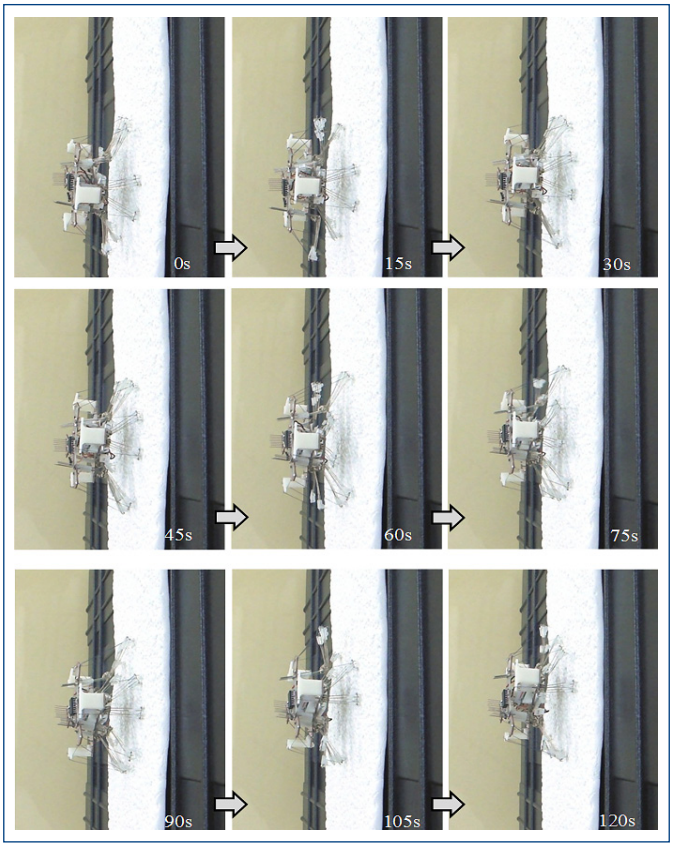

Figure 9. *Stroboscopic pictures during climbing on vertical wall with concave surface of P12*

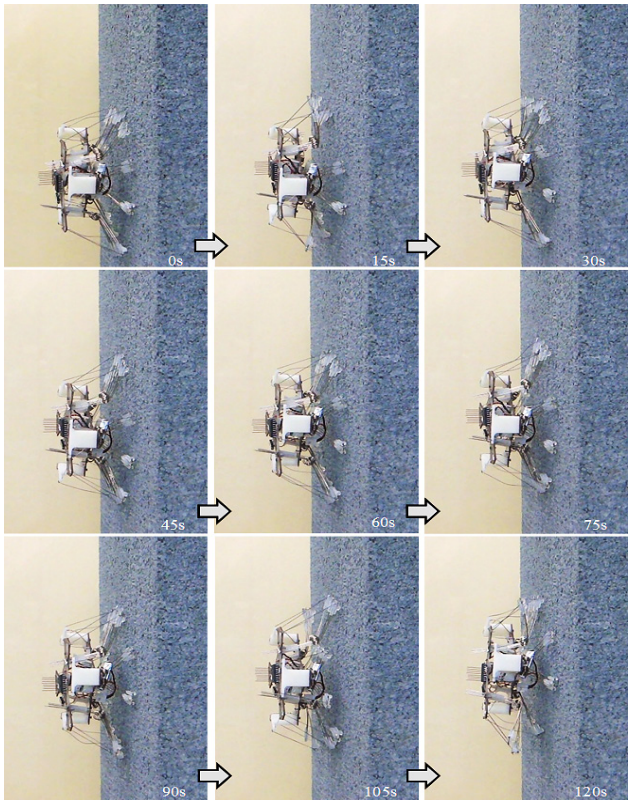

Figure 10. *Stroboscopic pictures during climbing on concrete wall*

climbing down, and horizontal travel were 0.30mm/s, 0.35mm/s, and 0.42mm/s (0.0035body length/s, 0.0041body length/s, and 0.0049 body length/s), respectively. This is due to the low response of the SMA spring cooling. Scaling down the robot improves the response of the SMA, since heat radiation and heat generation are proportional to the surface area, i.e., the length squared,and the volume, i.e., the length cubed, respectively. The speeding up in addition to the traveling direction change isour future work. Note that the robot was able to climb on thewall sloping at 70deg in the case of P16, 50deg in the case of P24, and 40deg in the case of P30.

Finally, to investigate the feasibility of this robot, we performed the concrete wall climbing experiment. Figure 10shows the stroboscopic pictures every 15s. The robot was able to successfully climb up, climb down, and travel horizontally on the vertical concrete wall. Fig. 11 shows the enlarged surface of the concrete wall and claws of the

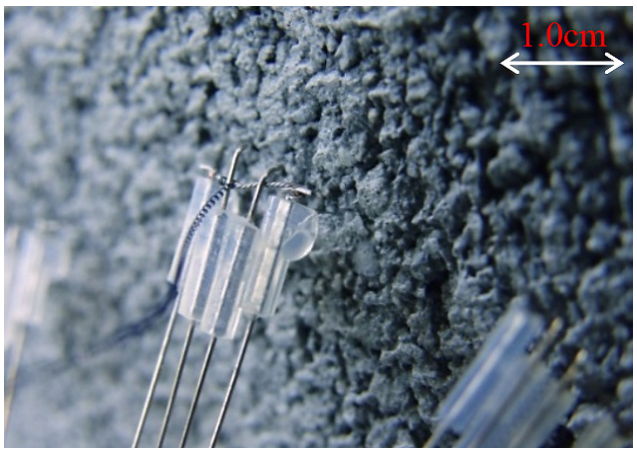

Figure 11. *Surface of concrete wall and claw of the robot*

robot. Common concrete walls have many holes of various diameters in addition to various offsets, i.e., various grain angles. The robot climbed by hanging the claws in holes equivalent to P12 or P14, i.e., grain angles of less than 30deg. Although the robot has two sets of eight claws for a leg, it cannot locomote on the wall in the case that there are no holes equivalent to P12 or P14 on the eight claw traveling trajectories. At least one claw out of the eight claws has to find a hole that can be gripped. In our future work, we intend to analyze the stochastic relationship between the claw number (in addition to their arrangement) and the wall adsorption ratio.

5. Conclusion

In this paper, we developed a cm-scale hexapod robot with claws to climb a vertical wall and investigated the relationship betweenthe grip using the claws of the leg and the surface properties of the wall theoretically and experimentally. The robot realized vertical and horizontal locomotion on a vertical concrete wall.

Agile locomotion, steering control, and an investigation into the relationship between the claw number, the claw trajectory, and the gripping of the wall are our future aims.

References

[Birkmeyer 2011] Birkmeyer, P.et al. CLASH: Climbing vertical Loose Cloth. Proceedings of the 2011 IEEE International Conference on Intelligent Robots and Systems, IEEE, 2011, pp.5087.

[Goran 2009] Goran A. et al. A Self-Exciting Controller for High-Speed Vertical Running. Proceedings of the 2009 IEEE/RSJ International Conference on Intelligent Robots and Systems, 2009, pp.631-638.

[Hirose 1992] Hirose, S. et al. Disk Rover: A Wall-Climbing Robot Using Permanent Magnet Disks. Proceedings of IEEE/RSJ International Conference on Intelligent Robots and Systems, 1992, pp.2074-2079.

[Kathryn 2008] Kathryn A. et al. A Body Joint Improves Vertical to Horizontal Transitions of a Wall-Climbing Robot. Proceedings of the 2008 IEEE International Conference on Robotics and Automation, 2008, pp.3046-3051.

[Kawasaki 2014] Kawasaki, S. and Kikuchi, K. Development of a Small Legged Wall Climbing Robot with Passive Suction Cups. Proceedings of the 3rd International Conference on Design Engineering and Science, 2014, vol. 2, pp. 112-116, ISBN 978-4-9905565-2-5

[Kim 2008] Kim, S., et al. Smooth Vertical Surface Climbing With Directional Adhesion. IEEE Transactions on Robotics, vol. 24, no.1, 2008, pp.65-74.

[Miyake 2008] Miyake, T. et al. Vacuum-based Wet Adhesion System for Wall Climbing Robots-Lubricating action and seal action by the liquid-. Proceedings of the 2008 IEEE International Conference on Robotics and Biomimetics, 2009, pp.1824-1829.

[Murphy 2007] Murphy, M.et al. Waalbot: An Agile Small-Scale Wall Climbing Robot Utilizing Pressure Sensitive Adhesives. IEEE/ASME Transaction on Mechatronics, vol.12, issue 3, 2007, pp.330-338.

[Suzuki 2010] Suzuki, K., et al. Insect-inspired Wall-climbing Robots Utilizing Surface Tension Forces. Journal of Advanced Mechanical Design, Systems, and Manufacturing, JSME, 2010, pp.383-390.

[Unver 2010] Unver, U. and Sitti, M. Flat Dry Elastomer Adhesives as Attachment Materials for Climbing Robots. Transactions on Robotics, vol. 26, no.1, 2010, pp.131-140.

[Yoneda 2001] Yoneda, K. et al. Development of a Light-weight Wall Climbing Quadruped with Reduced Degrees of Freedom. Proceedings of 4th International Conference on Climbing and Walking Robots, 2001, pp.907-912.

Contact:
prof. Koki Kikuchi
Department of Advanced Robotics, Chiba Institute of Technology
2 17 1, Tsudanuma, Narashino, Chiba, 275-0016, JAPAN
e-mail: kikut@ieee.org
URL: http://www.kikulab.it-chiba.ac.jp